Supplementary Information

Biogeochemical Dynamics of the Sea-Surface Microlayer from a Multidisciplinary Mesocosm Study

Authors:

Riaz Bibi[1]*, Mariana Ribas-Ribas[1], Leonie Jaeger[1], Carola Lehners[1], Lisa Gassen[1], Edgar Cortés[1], Jochen Wollschläger[1], Claudia Thölen[1], Hannelore Waska[1], Jasper Zöbelein[1], Thorsten Brinkhoff[1], Isha Athale[1], Rüdiger Röttgers[2], Michael Novak[2], Anja Engel[3], Theresa Barthelmeß[3], Josefine Karnatz[3], Thomas Reinthaler[4], Dmytro Spriahailo[4], Gernot Friedrichs[5], Falko Schäfer[5], Oliver Wurl[1]

1 Institute for Chemistry and Biology of the Marine Environment (ICBM), School of Mathematics and Science, Carl von Ossietzky Universität Oldenburg, Oldenburg, Germany

2 Helmholtz-Zentrum Hereon, Institute of Carbon Cycles, Geesthacht, Germany

3 GEOMAR Helmholtz Centre for Ocean Research Kiel, Kiel, Germany

4 Department of Functional and Evolutionary Ecology, University of Vienna, Vienna, Austria

5 Institute of Physical Chemistry, Kiel University, Kiel, Germany

Correspondence to: Riaz Bibi (riaz.bibi@uol.de)

The supplementary file includes:

Table S2 Average substrate color development (ASCD) values for 31 carbon substrates from Biolog EcoPlate™ incubations, used to assess microbial carbon utilization in SML and ULW samples (due to its length, it has been placed at the end of the Supplement to maintain readability).

Figure S9 Visualization of distribution patterns and contribution of individual nutrients to the components of SOM map**, (**a) NO_3^- (µmol L^{-1}), (b) NO_2^- (µmol L^{-1}), (c) $Si(OH)_4$ (µmol L^{-1}), (d) PO_4^{3-} (µmol L^{-1}), and (e) N:P ratio. The cells labeled 1, 2, and 3 on each component plane correspond to the identified clusters in the SOM, and the bold black cells indicate the contribution of nutrients to that cluster. The degree of contribution of each nutrient is visualized by the intensity of the color of the vertical bar (light color = high contribution, dark color = low contribution). Note that the vertical bars with numbers along each component present the degree of contribution and do not measure the values of nutrients.

Figure S10 Temporal dynamics demonstrate key biological and physical parameters coupling during the mesocosm period. (a) Chl*a* concentration indicating phytoplankton bloom progression, (b) distribution of the particles (5–10 µm and 3–4 µm, Cells ml^{-1}) for coccolithophores, and (c) albedo (%) exhibiting increased surface reflectance during coccolithophores bloom. The blue highlighted parts indicate the dates of nutrients addition (May 26, May 31 and June 1), the green highlighted part indicates the start date of the bloom phase (May 27), and the yellow highlighted part indicates the end date of the bloom phase (June 5).

Pilot study mixing experiment:

A mixing experiment was conducted with four set-up configurations of small flow pumps (ATK-4 Wavemaker 24V – 18 $m^3 h^{-1}$) in the SURF to determine the optimal configuration for a well-mixed basin with minimal capillary wave movement at the surface. Flow pumps were mounted on metal stands attached with metal clamps and hex jam nuts (Fig. S1) that could be loosened, opened, or closed to adjust the distance to the bottom of the SURF basin. Out of a total of eight flow pumps, one was placed in each corner of the basin facing towards the next corner, counterclockwise, and two were placed on each long side of the basin, close to the wall facing counterclockwise. Flow pumps had a digital touch controller to control and adjust the flow speed to make waves from 0 –100 in increments of 10. The flow angle of the pumps was also adjustable, and it was set to stay at an angle of 0° - 25° up, where 0° is the axis perpendicular to the metal stand and parallel to the ground.

A comprehensive set of measurements was carried out with a FerryBox (PocketBox, 4H-Jena) for the key parameters like phytoplankton biomass (Chlorophyll-a, Chl*a)* and turbidity to determine the homogeneity of the water column in SURF. The FerryBox inflow tube was inserted at different measuring points (Fig. S2) within the basin at the surface (about 20 cm depth) and at the bottom (about 30 cm off the ground). The exact measuring points within the basin were very similar for each configuration set-up and were always spread throughout the basin. The FerryBox measures every 5 s. Therefore, the duration of the inflow tube in the pool was set between 1–2 min to get an average value. The measurements of the configurations were then conducted after waiting at least an hour for the mixing process to occur. Table S1 displays the set-up configurations for the pumps and the obtained mean value, number of measurements, and standard deviation of the measured Chl*a* and turbidity values at all measured points. Initial ground state values of Chl*a* and turbidity were measured without any mixing actions with pumps before starting.

Figure S1 An image of one of the flow pumps mounted on the metal stand.

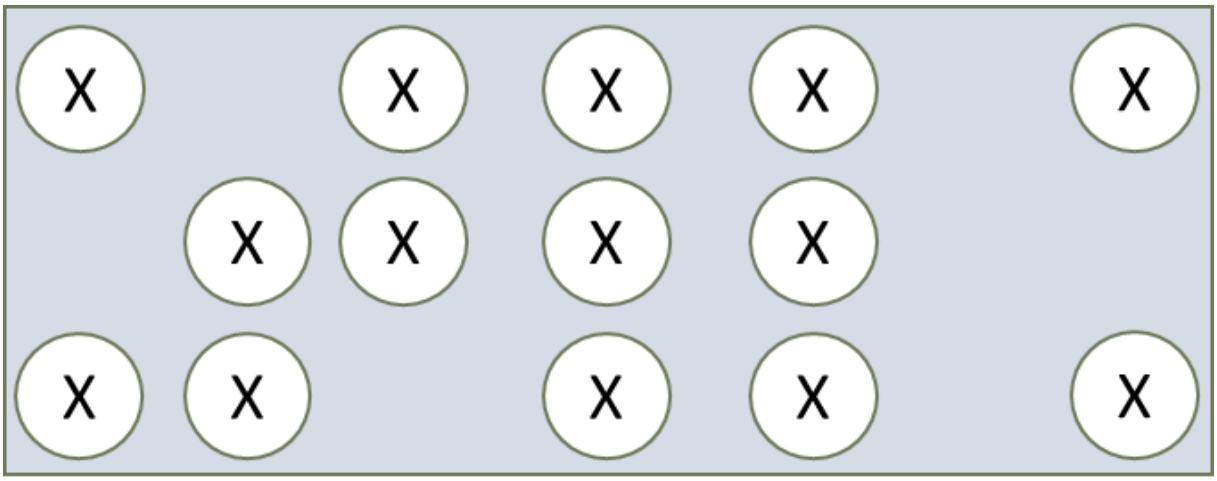

Figure S2 Schematic representation of measuring points of the FerryBox in SURF from a top-down perspective.

Table S1 Chl*a* and turbidity measured at different sampling points for different pumps configurations within the basin during the pilot phase. Their mean value (μ), number of measurements (N), and standard deviation (SD) are displayed together with the height, flow speed, and configuration of the pumps.

Configuration no.	**Height of pump on metal stand (23.5 cm)**	**Flow Speed of pump**	**Pump configuration in SURF pool**	**Chl*a*** **μ** **N** **SD**	**Turbidity** **μ** **N** **SD**
0	-	0	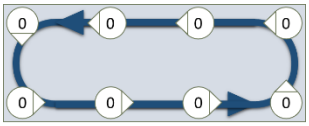	1.17 6 **0.06**	278.79 4 **214.89**
1	High	100	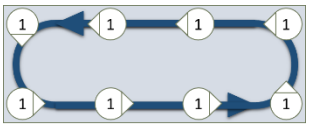	2.70 7 0.05	116.42 7 **2.25**
2	Low	10	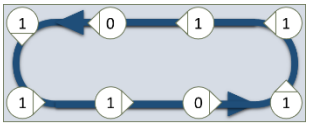	3.44 9 **0.11**	106.28 9 **0.38**
3	Low	10	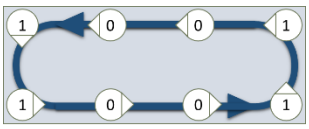	2.87 20 **1.43**	207.29 19 **112.33**
4	Low	20	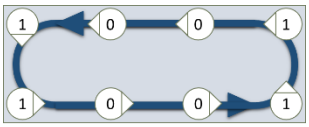	1.88 12 **0.09**	122.34 12 **68.09**

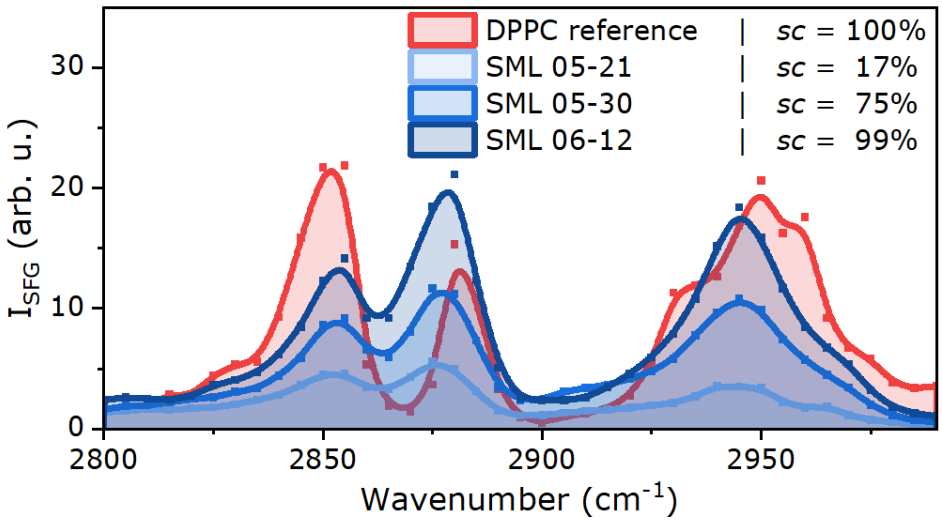

Figure S3 Exemplary data for the determination of the surface coverage index, *sc*. Three VSFG spectra of mesocosm samples with increasing *sc* value in comparison with the reference spectra of a DPPC (dipalmitoylphosphatidylcholine) monolayer with a surface concentration of 0.22 nmolcm^{-2}.

Surfactant Coverage Index:

Spectral signatures of C-H stretch vibrations in vibrational sum-frequency generation (VSFG) spectra can be used for quantification of surface-active molecules with alkyl chain functionalities. Referencing the measured spectral intensity to the VSFG spectrum of a well-defined monolayer of a reference with complete surface coverage allows one to define a *surface coverage* index *sc*. The operationally defined sum parameter *sc* is useful to characterize the state of natural air-water interfaces with respect to the effective coverage with surface-active organic substances, which plays a key role in describing the influence of surfactants on wave-damping and thus air-sea gas exchange. In contrast to the already widely used *surfactant concentration* (or *surfactant activity*) parameter, which is a measure for surfactant abundance in the entire SML on a micrometer scale (AC voltammetry, expressed in terms of µg Triton X-100 equivalent L^{-1}, µg Teq L^{-1}), the surface coverage index characterizes the presence of a molecular film of surfactants directly at the air-water interface on a nanometer scale. The use of VSFG for investigating the surface of natural water bodies has been pioneered by Koronowski et al. (1993) and has been further developed for SML characterization by Friedrichs and coworkers (Laß et al., 2011; Laß et al., 2011; Lange, 2021), including applications in SML time-series measurements (Laß et al., 2013) and the study of the microbial control of the SML surfactant state (Engel et al., 2018).

VSFG spectroscopy is a non-linear laser spectroscopic method to investigate molecular films at interfaces (Buck and Himmelhaus, 2001). It is inherently surface-sensitive due to the underlying spectroscopic selection rules of sum frequency generation (SFG) and only probes molecules present directly at the air-water interface on a molecular scale. In simple terms, SFG is the combination of two photons, one resonant with a molecular vibration, yielding a third photon that is detected as the signal. This non-linear process can only occur in a non-inversion symmetric environment, hence explaining the surface sensitivity of the method. Only molecules with preferential molecular alignment at the interface yield signal, where SFG signal intensity is proportional to the square of the second-order susceptibility $\chi^{(2)}$, $I_{SFG} \propto (\chi^{(2)})^2$. It can be interpreted as the macroscopic average of the molecular hyperpolarizabilities β such that the overall SFG intensity is proportional to the number of probed SFG active

molecules N squared: $I_{SFG} \propto \beta \times N^2$. Next to the N^2 dependence, due to changes of the overall molecular orientation of the probed molecules, β may depend on the surfactant surface concentration as well. However, it has been shown for natural SML samples that β and with it the measured spectral C-H signatures are largely independent of the surfactant abundance (Laß et al., 2011).

Therefore, the resulting square root relationship between N and the measured intensity leads directly to the operational definition of the surface coverage index:

$$sc = \frac{\sqrt{\int_{2800\ \mathrm{cm^{-1}}}^{3000\ \mathrm{cm^{-1}}} \left(\mathrm{I_{SML}}(\tilde{\nu}) - \mathrm{I_{H_2O}}(\tilde{\nu})\right) \mathrm{d}\tilde{\nu}}}{\sqrt{\int_{2800\ \mathrm{cm^{-1}}}^{3000\ \mathrm{cm^{-1}}} \left(\mathrm{I_{DPPC\ Reference}}(\tilde{\nu}) - \mathrm{I_{H_2O}}(\tilde{\nu})\right) \mathrm{d}\tilde{\nu}}}$$

Here, the nominator reflects the signal of the natural SML sample and the denominator the monolayer signal of the reference substance dipalmitoylphosphatidylcholine (DPPC) with a surface concentration of 0.22 nmol/cm^2 (corresponding to a surface pressure of 3.0 mN m^{-1}), representing the state of a 100 % covered surface. Both are corrected for the residual signal of a surfactant-free water background spectrum. In this way, surface coverage index values of sc = 0 % or sc = 100 % can be interpreted as a surfactant-free or a fully covered molecular film of surfactant-like material directly at air-water interface, respectively.

Example spectra are shown in Fig. S10 for three SML samples with increasing surface coverage values in comparison with the spectrum of the DPPC reference. Measurements of the SML samples were conducted in a circular Teflon dish with a surface area of 20 cm² and a spectral resolution of 5 cm^{-1}, and the DPPC sample has been analyzed with a Langmuir trough with the surface pressure measured using a Wilhelmy balance. Details of the commercial picosecond VSFG spectrometer (EKSPLA, 532 nm up-conversion wavelength) can be found in Laß and Friedrichs (2011) and Engel et al. (2018). Note that the spectra of the SML samples in Fig. S10 show different overall signal intensity, but the relative signal intensities of the observed vibrational bands remain largely unchanged, supporting that possible intensity variations related to β are minor (see above). In contrast to well-defined monolayers of single insoluble (dry) surfactants or soluble (wet) surfactants (the latter in adsorption equilibrium with the underlying bulk phase), natural surface films can be considered mixed films with contributions from different biosurfactants, biopolymers, and colloids forming complex interfacial structures.

145

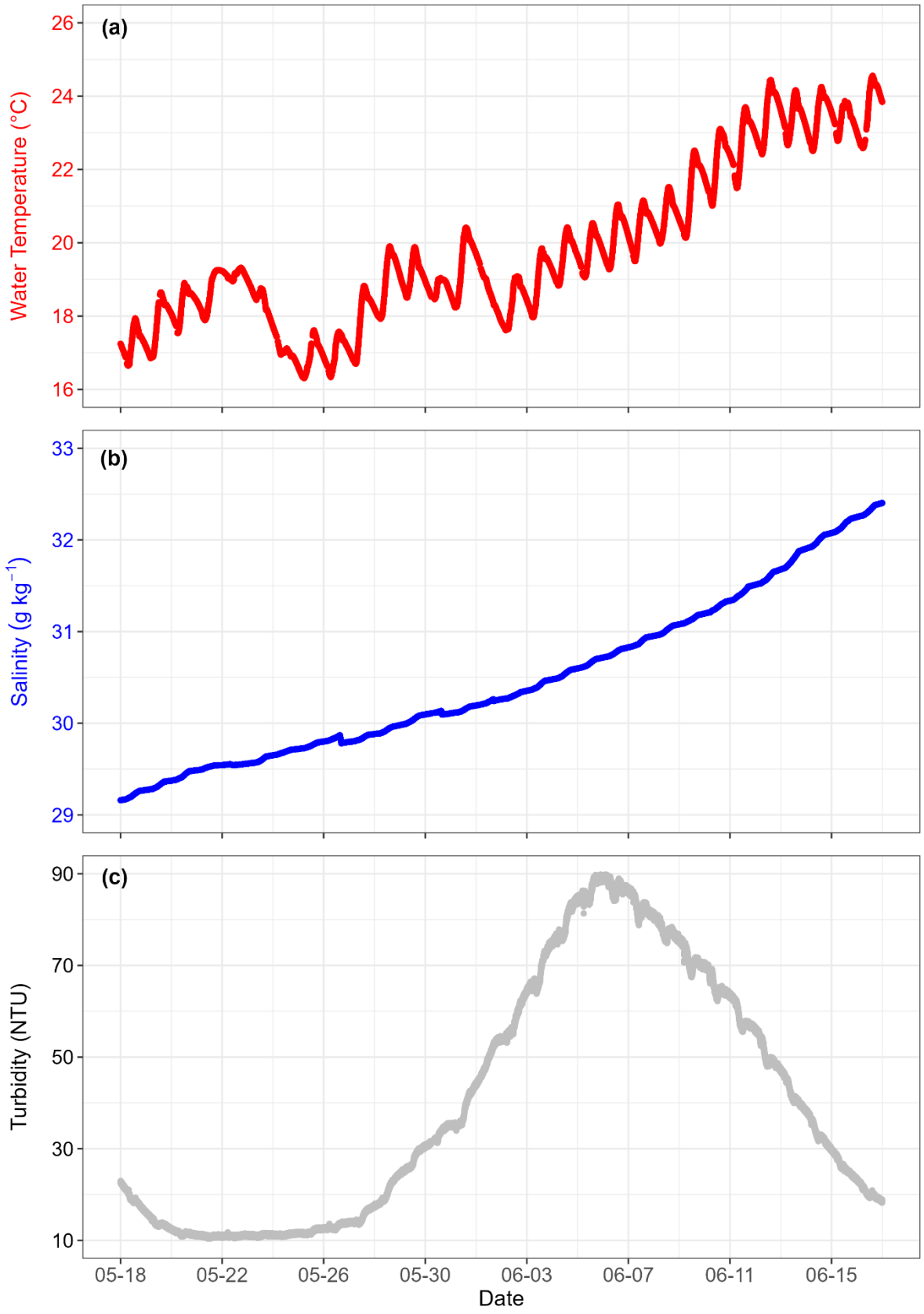

146

147 **Figure S4 Time series of continuous measurements for (a) water temperature (ºC), (b) salinity (g kg⁻¹), and**
148 **(c) turbidity (NTU).**

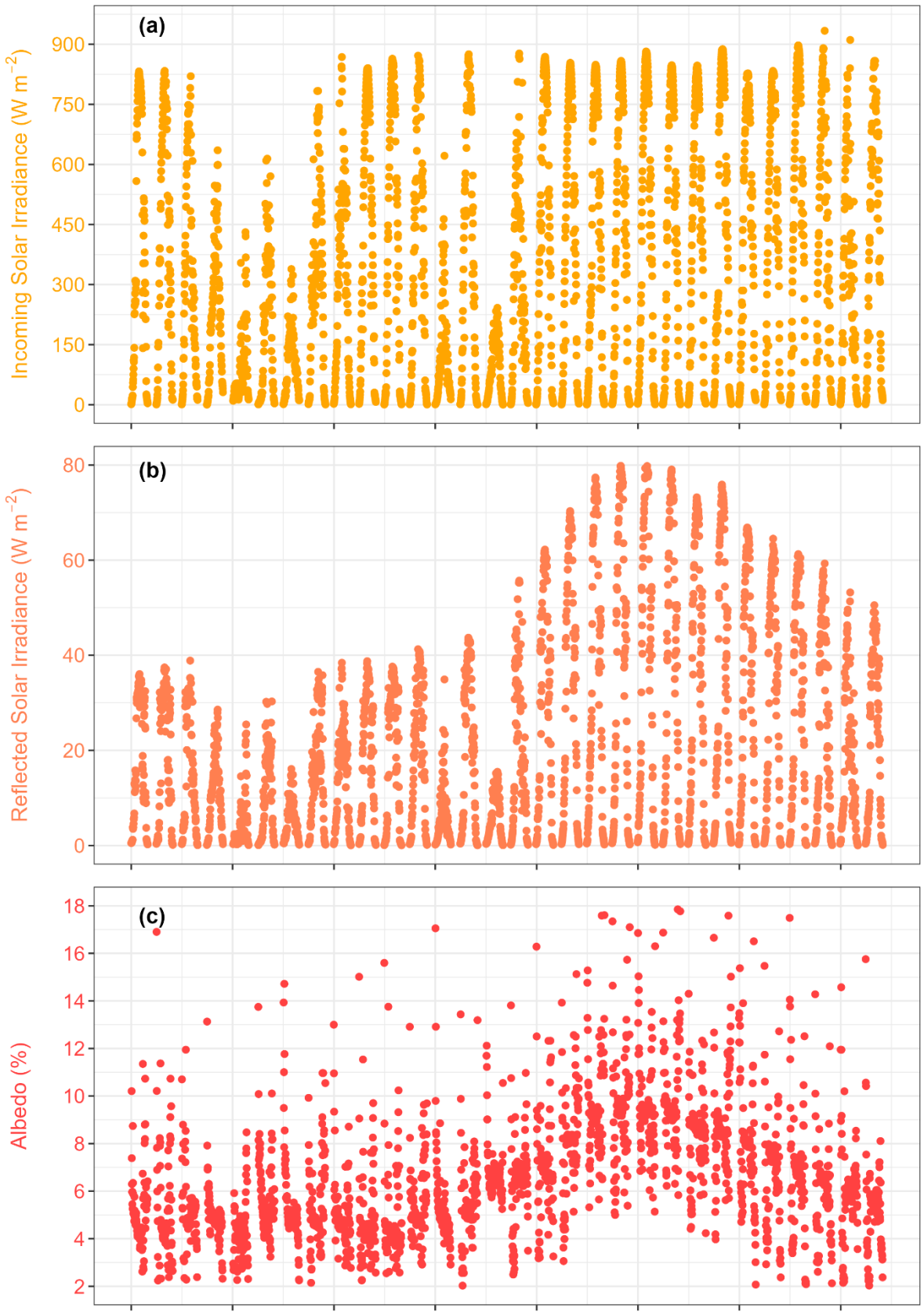
(a)
Incoming Solar Irradiance (W m^{-2})
900
750
600
450
300
150
0
(b)
Reflected Solar Irradiance (W m^{-2})
80
60
40
20
0
(c)
Albedo (%)
18
16
14
12
10
8
6
4
2

149

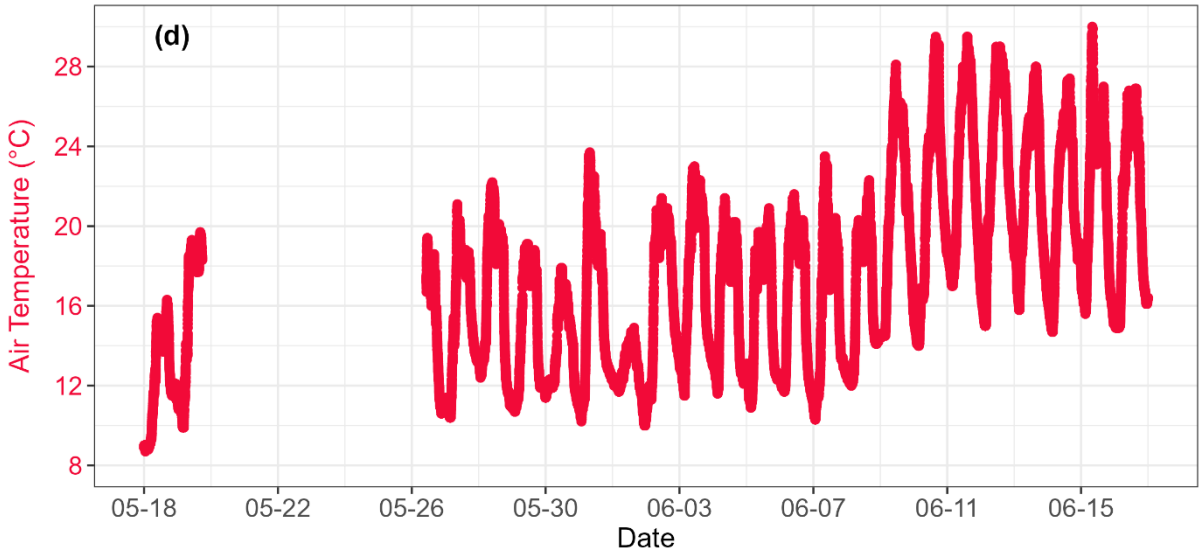

Figure S5 Time series of continuous measurements for (a) Incoming Solar Irradiance (W m^{-2}), (b) Reflected Solar Irradiance (W m^{-2}), (c) Albedo (%), and (d) Air Temperature (ºC), where gaps indicate days with missing air temperature records from the weather station.

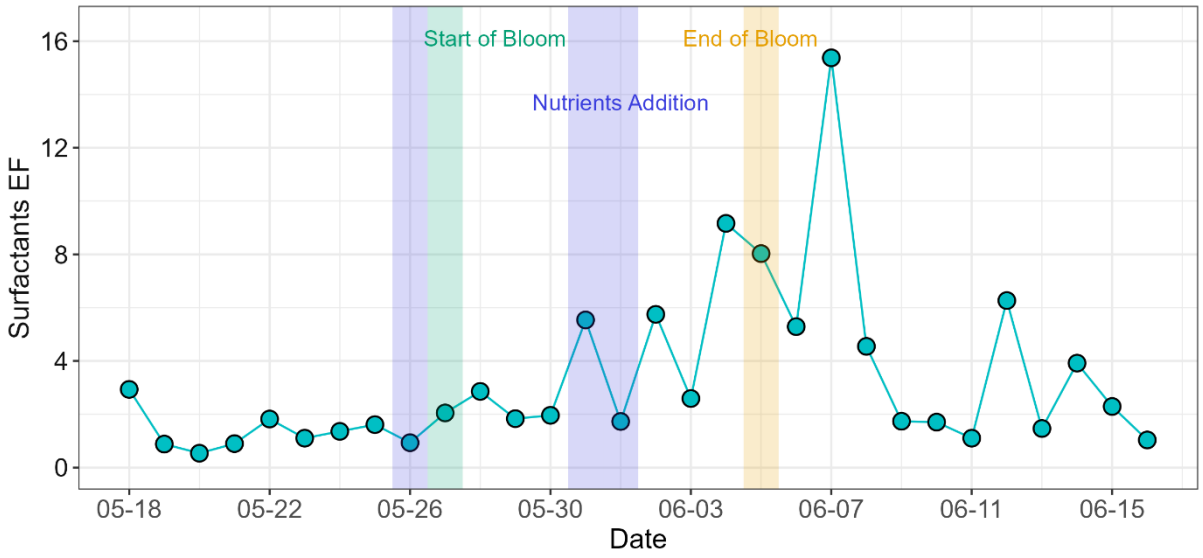

Figure S6 Temporal variation of surfactant enrichment factor (EF) during the mesocosm. The blue highlighted parts indicate the dates of nutrients addition (May 26, May 31, and June 1), the green

highlighted part indicates the start date of the bloom phase (May 27), and the yellow highlighted part indicates the end date of the bloom phase (June 5).

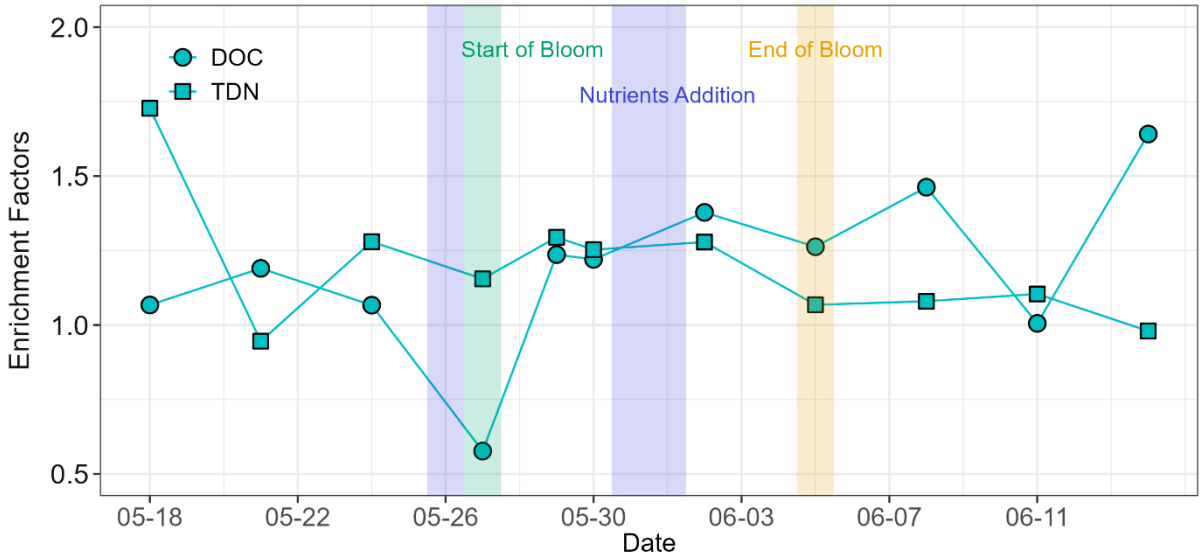

Figure S7 Time-series of DOC (circles) and TDN (squares) enrichment factors. The blue highlighted parts indicate the dates of nutrients addition (May 26, May 31, and June 1), the green highlighted part indicates the start date of the bloom phase (May 27), and the yellow highlighted part indicates the end date of the bloom phase (June 5).

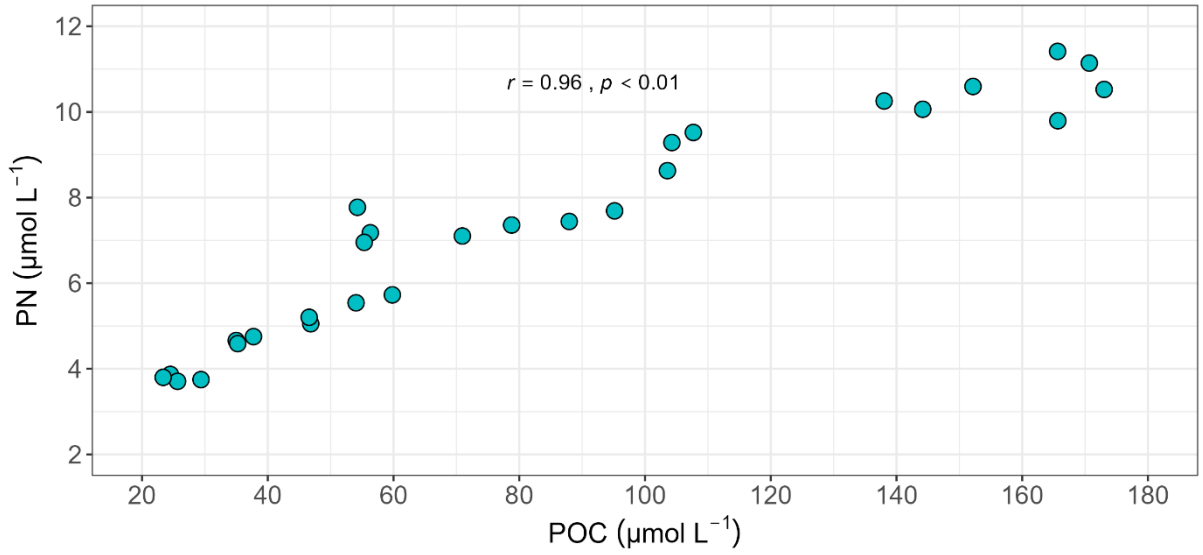

Figure S8 Correlation between POC and PN. A strong positive relationship between POC and PN (r = 0.96, p < 0.01), indicates a tight coupling of carbon and nitrogen dynamics over the time of mesocosm.

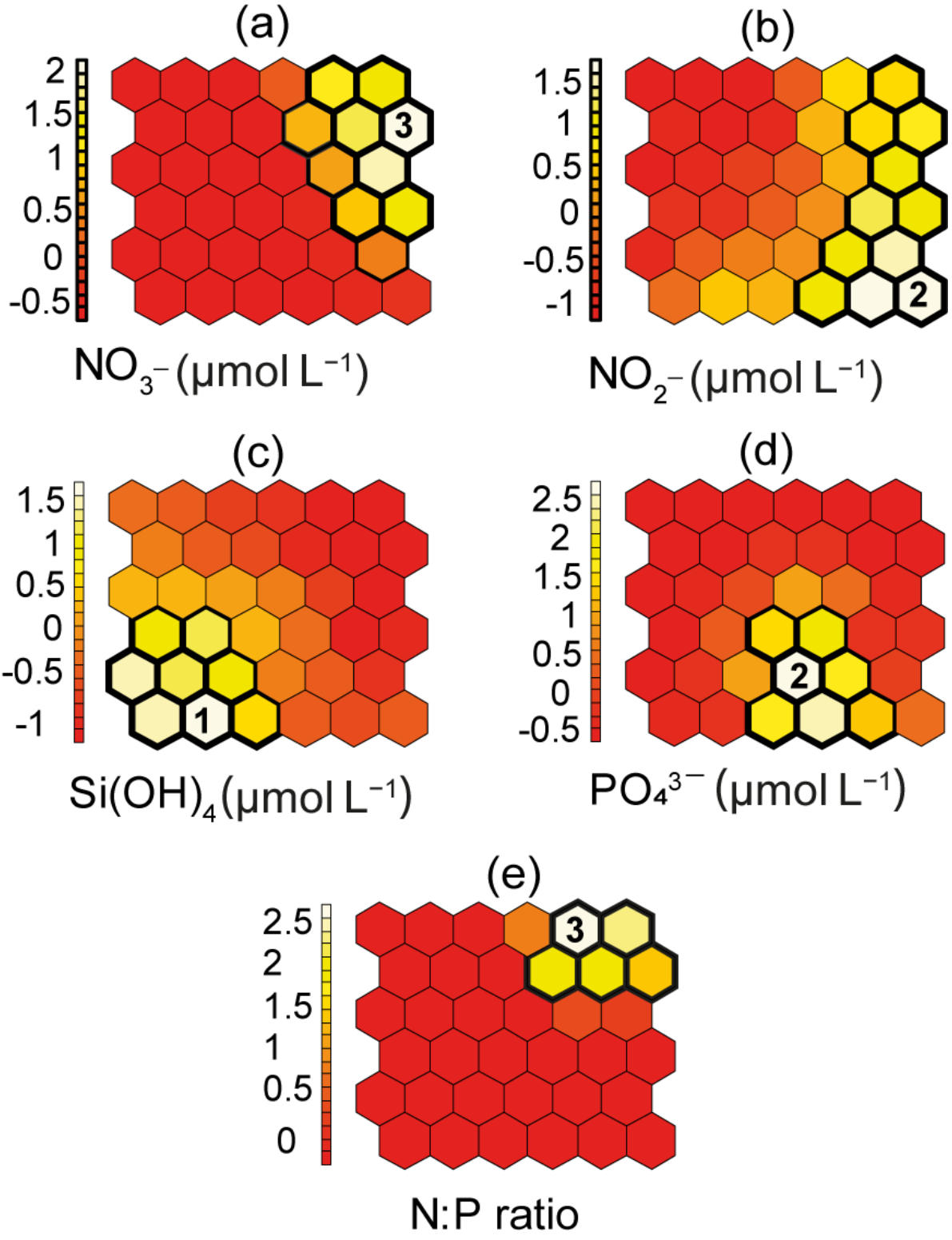

168

169 **Figure S9 Visualization of distribution patterns and contribution of individual nutrients to the components**
170 **of SOM map, (a) NO_3^- (μmol L^{-1}), (b) NO_2^- (μmol L^{-1}), (c) $Si(OH)_4$ (μmol L^{-1}), (d) PO_4^{3-} (μmol L^{-1}), and (e)**
171 **N:P ratio. The cells labeled 1, 2, and 3 on each component plane correspond to the identified clusters in the**
172 **SOM, and the bold black cells indicate the contribution of nutrients to that cluster. The degree of**
173 **contribution of each nutrient is visualized by the intensity of the color of the vertical bar (light color = high**
174 **contribution, dark color = low contribution). Note that the vertical bars with numbers along each**
175 **component present the degree of contribution and do not measure the values of nutrients.**

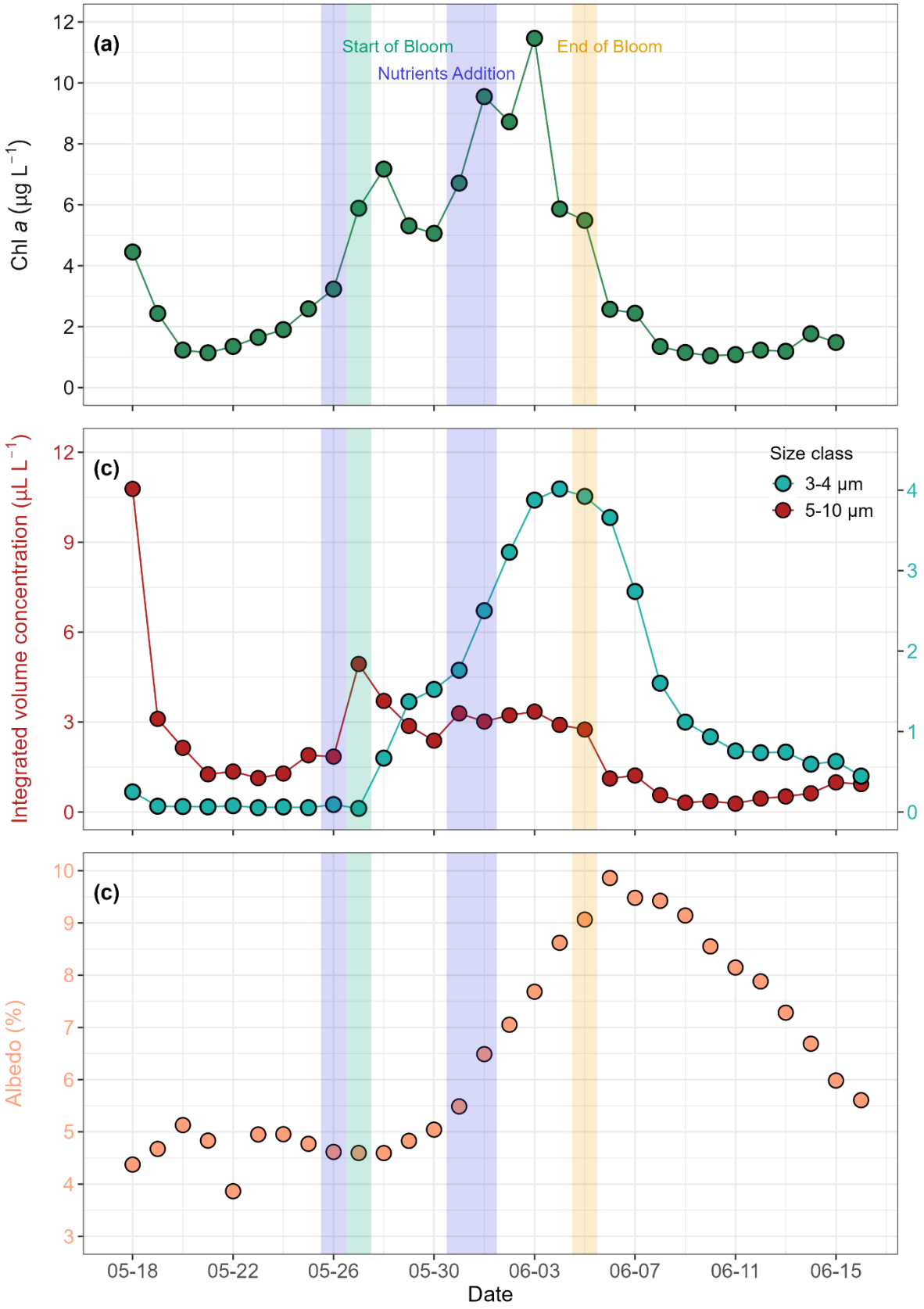

Figure S10 Temporal dynamics demonstrate key biological and physical parameters coupling during the mesocosm period. (a) Chl*a* concentration indicating phytoplankton bloom progression, (b) distribution of the particles (5–10 µm and 3–4 µm, Cells ml^{-1}) for coccolithophores, and (c) albedo (%) exhibiting increased surface reflectance during coccolithophores bloom. The blue highlighted parts indicate the dates of

nutrients addition (May 26, May 31 and June 1), the green highlighted part indicates the start date of the bloom phase (May 27), and the yellow highlighted part indicates the end date of the bloom phase (June 5).

Refrences

Buck, M., and Himmelhaus, M.: Vibrational spectroscopy of interfaces by infrared-visible sum frequency generation. J. Vac. Sci. Tech. A, 19, 2717-2736, 2001.

Engel, A., Sperling, M., Sun, C., Grosse, J., and Friedrichs, G.: Organic matter in the surface microlayer: Insights from a wind wave channel experiment, Frontiers in Marine Science, 5, 182, 2018.

Korenowski, G. M., Frysinger, G. S., and Asher, W. E.: Noninvasive probing of the ocean surface using laser-based nonlinear optical methods. Photogramm. Eng. Rem. Sens., 59, 363-369, 1993.

Lange, F.: Investigation of Sea Surface Nanolayer Properties and Photochemistry Using Modern Laser Spectroscopic and Surface Analytical Techniques, Dissertation, https://nbn-resolving.org/urn:nbn:de:gbv:8:3-2021-00564-5, Kiel University, 2021.

Laß, K., Kleber, J., and Friedrichs, G.: Vibrational sum-frequency generation as a probe for composition, chemical reactivity, and film formation dynamics of the sea surface nanolayer. Limnol. Oceanogr.: Methods 8, 216-228, 2010.

Laß, K., Friedrichs, G.: Revealing Structural Properties of the Marine Nanolayer from Vibrational Sum Frequency Generation Spectra. J. Geophys. Res. 116, C08042, 2011.

Laß, K., Bange, H., and Friedrichs, G.: Seasonal signatures in SFG vibrational spectra of the sea surface nanolayer at Boknis Eck Time Series Station (SW Baltic Sea). Biogeosciences,10, 5325-5334, 2013.

Table S2 Average substrate color development (ASCD) values for 31 carbon substrates from Biolog EcoPlate™ incub

Date	Depth	beta-Methyl-D-Glucoside	D-Galactonic Acid gamma lactone	L-Arginine	Pyruvic Acid Methyl Ester	D-Xylose	D-Galacturonic Acid	L-Asparagine
5/23/2023	SML	0.25	0.11	1.46	1.13	0.04	1.51	1.28
5/23/2023	ULW	1.24	0.88	1.39	0.98	0.36	1.03	1.26
5/26/2023	SML	0.47	0.64	1.06	1.59	0.10	1.31	1.65
5/26/2023	ULW	-0.03	0.25	0.91	2.15	0.30	0.07	1.36
5/27/2023	SML	0.82	0.23	1.12	1.07	0.42	1.20	1.40
5/27/2023	ULW	-4.61	26.18	-12.65	-11.38	30.59	11.37	-26.70
5/30/2023	SML	0.24	0.41	1.16	1.24	0.24	1.35	1.73
5/30/2023	ULW	1.26	0.83	1.16	1.08	0.91	1.10	0.86
5/31/2023	SML	1.15	0.92	0.81	1.12	0.59	1.09	1.40
5/31/2023	ULW	2.85	7.75	3.43	-0.98	3.89	-2.99	-1.78
6/3/2023	SML	0.73	1.06	1.07	1.12	1.09	1.09	1.19
6/3/2023	ULW	0.76	0.97	1.43	2.90	0.42	0.86	1.19
6/4/2023	SML	0.74	0.78	1.19	1.11	0.81	1.03	1.32
6/4/2023	ULW	1.19	0.97	1.05	2.23	1.00	1.09	1.48
6/7/2023	SML	0.81	1.05	1.07	0.62	1.57	1.34	0.67
6/7/2023	ULW	0.85	1.94	2.06	5.78	0.17	0.44	1.45
6/8/2023	SML	0.74	1.06	1.10	0.90	0.78	1.38	1.71
6/8/2023	ULW	0.59	0.95	1.04	0.96	0.21	1.13	0.91
6/11/2023	SML	0.53	1.58	1.42	0.43	1.03	0.51	1.70
6/11/2023	ULW	0.68	0.98	1.07	2.28	0.34	0.63	1.00
6/12/2023	SML	0.61	1.34	1.23	0.96	0.79	0.43	1.85
6/12/2023	ULW	0.00	1.57	1.42	1.99	-0.21	0.37	2.64

ıations, used to assess microbial carbon utilization in SML and ULW samples. Negative values reflect negligible or no s

Tween 40	I-Erythritol	2-Hydroxy Benzoic Acid	L-Phenylalanine	Tween 80	D-Mannitol	4-Hydroxy Benzoic Acid	L-Serine	alpha-Cyclodextrin
1.18	1.14	0.14	0.35	1.21	1.70	0.51	1.70	2.45
1.37	0.79	0.46	0.87	0.52	3.15	0.25	1.18	2.34
1.17	0.26	-0.02	0.59	1.30	1.77	-0.03	2.05	2.02
1.32	-0.06	-0.18	0.47	1.26	3.02	-0.67	2.11	3.69
1.33	0.88	-0.01	0.91	1.32	1.57	-0.05	1.85	1.57
0.90	10.58	14.74	11.04	8.52	-13.59	16.62	-17.45	-25.07
1.23	0.13	-0.01	0.98	0.88	2.10	-0.03	2.18	2.34
1.47	0.94	0.71	2.10	0.06	-0.28	2.30	0.61	2.32
1.20	1.15	-0.14	0.80	1.38	1.97	-0.18	1.41	1.94
12.45	5.48	8.25	-6.72	7.70	1.70	-11.40	3.02	2.68
1.19	1.04	-0.19	1.05	1.11	1.87	0.03	1.64	1.84
0.90	1.24	0.40	0.28	0.47	2.26	-0.49	1.55	3.34
0.98	1.24	0.03	0.38	1.29	1.73	0.63	1.35	1.57
0.88	0.45	0.26	1.19	0.80	1.49	-0.10	1.36	1.21
1.22	1.06	-0.11	0.15	1.16	2.10	0.86	1.27	2.00
1.55	0.47	1.20	0.36	-0.97	0.78	-1.41	0.50	3.12
1.17	0.56	-0.02	1.10	1.37	1.90	-0.11	1.73	1.69
1.23	0.14	-0.13	0.91	0.50	1.86	0.26	1.63	2.64
1.64	0.31	-0.06	1.12	1.62	2.32	0.13	1.22	1.53
0.93	0.59	-0.06	0.93	0.81	2.73	0.55	1.10	2.28
1.23	0.09	-0.15	0.55	1.22	2.25	-0.16	1.87	2.27
0.84	0.96	-0.88	-1.97	0.05	1.40	-2.78	2.87	5.59

substrate use and were retained for transparency.

N-Acetyl-D-Glucosamine	gamma-Hydroxybutyric Acid	L-Threonine	Glycogen	D-Glucosaminic Acid	Itaconic Acid	Glycyl-L-Glutamic Acid	D-Cellobiose	Glucose-1-Phosphate
1.79	0.86	1.76	1.91	0.35	1.15	1.47	1.50	0.58
0.66	0.08	1.70	3.32	0.78	0.10	1.58	1.69	0.51
1.97	0.92	1.26	1.80	0.15	0.75	1.42	2.26	1.18
3.74	0.48	1.35	3.22	0.08	0.85	0.52	1.70	0.31
1.81	1.15	1.83	1.62	0.11	0.15	1.55	1.88	1.20
-16.81	38.98	-16.09	-49.17	-2.50	9.40	-14.46	-12.10	30.93
2.08	1.40	1.78	1.94	0.23	0.23	1.42	1.87	1.35
0.36	2.72	1.85	0.87	-0.34	1.07	0.06	2.23	1.11
1.65	1.48	1.94	1.43	0.23	0.46	1.34	1.61	1.04
-4.27	-5.07	3.93	4.01	5.56	-1.26	3.74	4.90	-2.68
1.50	1.63	1.69	1.51	0.20	0.60	1.18	1.67	1.38
1.03	0.95	1.05	3.04	0.17	-0.59	0.95	0.97	0.95
1.34	1.46	1.74	1.05	1.11	1.03	1.16	1.39	1.01
1.33	0.25	1.49	2.65	0.73	0.59	1.00	1.97	1.45
1.64	1.35	1.84	1.03	0.35	1.06	1.11	1.08	0.91
3.84	-3.07	1.57	5.02	0.76	0.13	0.39	1.19	0.90
1.76	1.21	1.94	1.16	0.09	0.29	1.35	1.50	0.97
2.01	0.69	1.43	2.48	0.56	1.04	0.92	1.58	1.24
1.81	1.79	1.85	1.29	0.08	0.28	1.36	1.54	0.53
2.05	0.23	1.13	2.37	0.78	0.64	0.96	0.67	0.94
1.88	1.19	2.27	1.53	-0.05	0.48	1.48	1.70	1.18
3.17	-2.47	1.89	5.90	-1.13	-0.33	0.57	1.84	2.19

alpha-Ketobutyric Acid	Phenylethyl-amine	alpha-D-Lactose	D,L-alpha-Glycerol Phosphate	D-Malic Acid	Putrescine
0.76	-0.04	0.87	0.61	0.50	0.80
-0.04	-0.35	0.49	0.50	1.19	0.71
0.23	0.01	0.29	0.60	0.88	1.34
0.14	-0.12	0.96	0.95	0.01	0.85
0.39	0.07	0.59	0.65	0.98	1.39
29.02	9.78	18.89	2.44	-12.71	-3.69
0.24	0.05	0.04	0.63	0.22	1.34
1.25	0.82	-0.48	0.22	0.01	1.83
0.26	0.01	0.95	0.51	0.21	1.29
-4.50	-4.33	-6.35	-0.28	4.29	-2.02
0.21	0.26	-0.02	0.51	0.43	1.32
0.31	0.18	0.58	1.26	0.71	0.98
0.32	0.35	0.49	0.37	0.76	1.26
0.49	-0.06	0.08	0.85	0.41	1.23
0.10	-0.05	1.04	0.55	1.03	1.12
-1.50	0.30	0.76	1.00	0.61	0.82
0.30	0.22	0.51	0.47	0.98	1.19
0.53	0.13	0.82	1.32	0.56	0.87
0.22	0.22	0.78	0.23	0.70	1.29
0.49	0.32	0.52	0.94	0.95	1.18
0.13	-0.19	0.34	0.35	1.02	1.30
0.82	-0.73	0.57	0.44	0.62	3.77